
Article:
Miao, Q, Zhang, M, McDaid, A et al. (2 more authors) (2020) A robot-assisted bilateral upper limb training strategy with subject-specific workspace: A pilot study. Robotics and Autonomous Systems, 124. 103334. ISSN 0921-8890

https://doi.org/10.1016/j.robot.2019.103334

A robot-assisted bilateral upper limb training strategy with subject-specific workspace: A pilot study

Qing Miao[1,2], Mingming Zhang[1,2]*, Andrew McDaid[2], Yuxin Peng[3], Sheng Q. Xie[2]

[1] Department of Biomedical Engineering, Southern University of Science and Technology, Shenzhen, China
[2] Department of Mechanical Engineering, the University of Auckland, Auckland, New Zealand
[3] Department of Physical Education and Sports Science, Zhejiang University, Hangzhou, China
*Corresponding Author at zhangmm@sustech.edu.cn

Abstract—This paper proposes a new robot-assisted bilateral upper limb training strategy, focusing on the bilateral coordination *of users' upper limbs.* The strategy is implemented and evaluated on a bilateral upper limb rehabilitation device (BULReD) that is an H-bot mechanism actuated by two Maxon DC motors. The control system consists of a position controller, an admittance controller and an adaptive algorithm, where the BULReD stiffness is modified session by session based on training performance. This strategy is also integrated with subject-specific workspace for enhanced training safety. Experiments were carried out with five subjects through active reaching tasks. Results indicate that the proposed training strategy requires significant coordination of bilateral upper limbs for task completion, and is able to tune control parameters to *an appropriate difficulty level based on participants' training* performance. Future work will focus on its clinical evaluation on patients with upper limb disabilities.

Keywords: Robot-assisted, bilateral, upper limb, training strategy, subject-specific workspace.

I. INTRODUCTION

While longitudinal studies suggest that 30% to 66% of stroke survivors do not have full arm function six months post-stroke [1], evidence has suggested that upper limb motor skills can be improved by following rehabilitation interventions [2-4]. Various upper limb rehabilitation robotic systems have been developed and used with many kinds of patients with disabilities over the past few decades [5-8], with promising clinical efficacy, for example on MIT-Manus and ARMin III systems. Ang, et al. [9] used MIT-Manus combined with electroencephalography-based motor imagery brain-computer interface technology through a randomized controlled trial on 26 hemiplegic subjects and achieved positive results. Klamroth-Marganska, et al. [10] delivered ARMin III robotic training system on 38 patients with motor impairment for over six months, where results showed improvements in terms of Fugl-Meyer assessment (FMA) score.

Existing robotic systems for upper limb rehabilitation can be classified into unilateral and bilateral devices. Brackenridge, et al. [6] reviewed a variety of upper limb robotic systems with more unilateral ones than bilateral ones, including experimental prototypes and commercial products. It can be inferred that robot-assisted unilateral training technology is relatively mature for upper limb rehabilitation, some of them being currently used in rehabilitation clinics and hospitals. However, some studies have suggested that bilateral training has promising improved clinical efficacy, especially when used for coordination training. Summers, et al. [11] found significant improvements in a short-term bilateral versus unilateral training study with mildly impaired subjects. Stoykov, et al. [12] showed superior outcomes with long-term bilateral training with subjects who were much more impaired. Medical literature also supports bilateral rehabilitation training to activate the primary motor cortex and supplementary motor area of the intact limb. This can increase the likelihood of voluntary muscle contractions of the impaired limb when symmetrical movements are executed [13].

Robot-assisted bilateral upper limb training systems can be generally classified into three configuration categories: two independent robotic devices [14-18], one robotic device with an assistive system (EMG-based as an example) [19, 20], and one device with two handles [21-23].The two-independent-device bilateral system is generally able to achieve different kinds of training modes [24], including joint space symmetry (mirror-image) [14-17, 19], visual symmetry [17, 18, 20, 22, 23], point mirror symmetry [21-23] and asymmetry [16, 17]. Examples are: Guo, et al. [14] implemented passive-mirroring on a single-arm robot in a master-slave configuration using an external haptic device. Rashedi, et al. [15] developed a robotic device using healthy hands to move the impaired side in mirror-image motion pattern. Lum, et al. [18] used a hand-object-hand system to achieve transport tasks that move a pencil-like object back and forth rhythmically to audible ticks. Stinear and Byblow [16] achieved an active-passive bimanual movement therapy by conducting wrist reaching tasks in both mirror symmetric and asymmetric (a phase lag of 60 degrees) pattern. Miao, et al. [17] used two different universal robots to achieve joint space symmetry, visual symmetry and asymmetric patterns for upper limb training.

The second category of robotic system is more frequently used for delivering joint space or visual symmetry coupled with an external assistive system. Leonardis, et al. [19] used the BRAVO hand exoskeleton system to achieve a mirror grasping tasks through an EMG-controlled system estimating the force of the non-paretic hand and transferring to the device. Lien, et al. [20] developed a bilateral training system containing an exoskeleton robot NTUH-II and an inertia motion unit to realize passive and active-assistive visual symmetry training. In general, it can be summarized that two-independent-device and one-device-one-assistive-system bilateral training systems predominantly focus on using healthy limbs to provide reference movements while the devices providing assistance or resistance to impaired limbs. While these robotic systems can implement various training modes, the requirement for active cooperation of human bilateral limbs for tasks is minimal.

In contrast, the third category of one-device-two-handle robotic systems [21-23] focus more on cooperation and

coordination training of bilateral limbs. Johnson, et al. [21] used the driver's SEAT providing assistance for the weak arm to complete point symmetric steering tasks based on EMG-measured force signals. Trlep, et al. [22] proposed training tasks which involved tracking an on-screen target by manipulating two handles on a Haptic Master robot. The handlebar orientation was used as control signals for virtual 4airplane movement, where the unaffected limb is scaled down using an adaptive gain to stimulate use of the paretic arm. Squeri, et al. [23] used the Braccio di Ferro to conduct reaching tasks where patients were required to move towards a target whilst keeping the bar at a predefined angle. The reinforcement learning scheme is expressed by means of suitable force fields rendered by the haptic device, adapting to the participant's performance. It is highlighted that comparing with the SEAT system for only rotational movement, the systems in [22, 23] enable translational and rotational movements (denoted as visual symmetry and point symmetry, respectively). However, they are expensive due to the use of Haptic devices and/or multi-axis load cells.

This study proposes a new robot-assisted bilateral upper limb training strategy with subject-specific workspace for training safety and efficacy [17]. It was implemented and evaluated with a previously developed bilateral upper limb rehabilitation device (BULReD) [25], and an adaptive admittance controller. This implementation is low cost and features random reaching targets within subject-specific workspace, as well as adaptation to training performance based on multiple variables. The paper is organized as follows: a detailed robot-assisted bilateral upper limb training system is described in section II which includes system configuration, training strategy, control system and subject-specific workspace determination. Experimental results with five healthy subjects are presented next, followed by Discussion and Conclusion.

II. Methods

A. System Configuration

The BULReD consists of three main components, namely the base module, the motion module, and the hand holder [25]. The base module acts as a foundation to support the motion module. The motion module consists of two mutually perpendicular linear slide systems, the bridge and the cart. The hand holder is rigidly connected with the cart through a three-axis force sensor. In this paper, the structure of the device installs an angle sensor under the hand holder to measure the angular position of the hand holder. To guarantee the safety of bilateral upper limb training, there are four main options included in the robotic system. Firstly, four limit switches are set up locating at the corner of the workbench to restrict the end-effector movement inside the robotic workspace. Secondly, a stop button is available to make the device out of active operation at any time. Thirdly, both handle bars are designed without hand constraints, so the participants can voluntarily hold or release them during the training. Finally, the presented strategy is based on admittance control, which is capable of making the human-robot interaction compliant.

A schematic diagram of the robotic layout is presented in Fig. 1, where the origin of global coordinate (OGC) is labelled and key dimensions are identified on a subject specific basis. Each participant is required to remain standing upright during the whole training process, ensuring a constant relative position with the robotic device. An average set of human segment lengths expressed as a percentage of body height is adapted as provided by Winter [26]. Considering the height of a subject as H, the height of shoulders $B = 0.818 * H$, the distance between shoulders $S = 0.259 * H$, the length of palm is $0.108 * H$, and other parameters $L_1 = 0.186 * H$, $L_2 = 0.146 * H$, $L_3 = 0.054 * H$ (estimated half of the palm size). In this study, we set $D_1 = 405\text{mm}$ as the distance on the Y-axis between OGC and the human body, and $D_2 = 1182\text{mm}$ as the height of OGC.

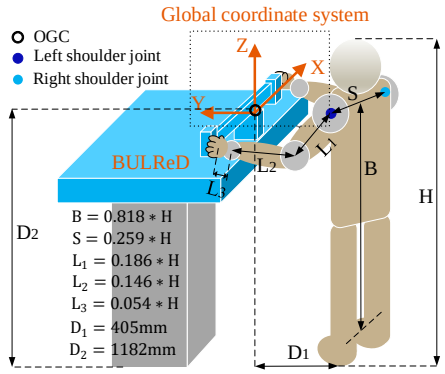

Fig.1: Schematic diagram of the robot-assisted bilateral upper limb training system. (The orange arrowed lines refer to the global coordinate system.)

B. Training Strategy

The newly proposed robot-assisted bilateral upper limb training strategy with subject-specific workspace, is presented in Fig.2. The black square represents the workspace of the BULReD whose X axis ranges between $[-160\text{mm}\ 160\text{mm}]$, and Y axis between $[0\text{mm}\ 320\text{mm}]$. The grey irregular closed curve is the feasible workspace boundary (FWB), which is a function of a specific participant's body size. The black dot denotes the start point P_s of training trajectory, and the red ones are training targets (Target_1, Target_2,…, Target_n). The arrowed red line represents the desired training trajectory. The blue bar represents the handle holder. The virtual tunnel line with red shadow (VT_L) and the virtual tunnel angle with blue shadow (VT_A) are denoted as training trajectory and angle, respectively. The green dashed line is parallel to X axis. The black dashed line represents the desired angular position θ_d of the hand holder, and the blue one represents its measured angular position θ. Parameters Q_{thr} and Θ_{thr} correspond to VT_L and VT_A, respectively.

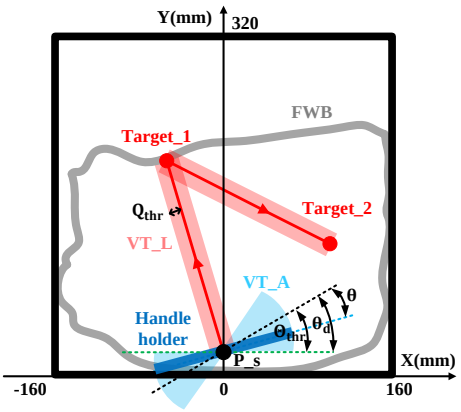

Fig.2: Schematic diagram of the proposed training strategy. (The grey irregular closed curve represents the feasible workspace boundary (FWB). The black dot P_s is the start point of the training trajectories. Regions VT_L and VT_L represent Q_{thr} and Θ_{thr}, respectively. The parameter θ_d is desired angular position, and θ is measured angular position.)

The proposed training strategy includes three main steps: 1) determining the subject-specific workspace and random task target distribution; 2) manipulating the handle holder at θ_d in a virtual angle tunnel, and moving the handle holder towards the task target along a virtual path tunnel within a desired time period t_d; and 3) generating another random dot target within appropriate workspace for a new round in the same session of training when the current target is reached.

C. Control System with Adaptation

To enable the BULReD to implement the proposed training strategy, a control system is developed consisting of an admittance controller, a position controller module, and an adaptive law based on training performance, as presented in Fig.3.

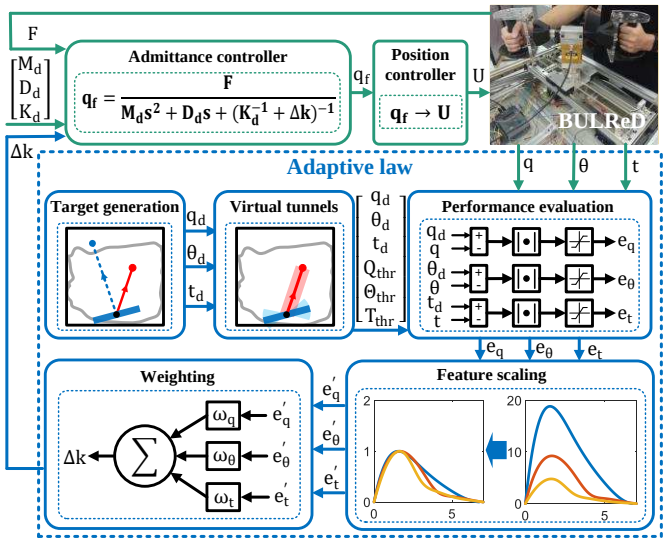

Fig.3: Control diagram of the BULReD. (The parameters M_d, D_d and K_d are the inertia, stiffness and damping parameters, respectively. The measured force F is from the participant. The output of the admittance controller q_f is the increased position, and the input of the position controller U is the input voltage for motors. For the adaptive law, the parameters e_q, e_θ and e_t are performance evaluation indicators corresponding to position, angle and time deviation. After feature scaling, the gain Δk is calculated by weighting.)

Admittance control makes the device operate with a specific inertia, damping and stiffness by measuring and controlling the force from the force sensor. The admittance equation is written as in (1).

$$q_f = \frac{F}{M_d s^2 + D_d s + (K_d^{-1} + \Delta k)^{-1}} \quad (1)$$

Here, $F = [F_x \quad F_y]^T$ is denoted as the measured interaction force vector along X axis and Y axis, M_d, D_d and K_d represent the desired inertia, damping and stiffness, respectively. The gain value Δk is calculated by adaptive law. Setting $q_f = [X_f \quad Y_f]^T$ as the increased position vector corresponding to F, the admittance law can be simplified into (2) as a linear spring, where $M_d = D_d = 0$.

$$q_f = \frac{F}{(K_d^{-1} + \Delta k)^{-1}} \quad (2)$$

Considering the specification of the electric motors, a position controller is used to convert q_f into required motor voltage $U = [U_1 \quad U_2]^T$, which can be obtained in (3),

$$U = \frac{60}{2\pi} R q_f \gamma v_t^{-1} t^{-1} \quad (3)$$

where $R = r^{-1}\begin{bmatrix} 1 & 1 \\ 1 & -1 \end{bmatrix}$ as the inverse kinematic matrix, r denoted as the radius of the pulley. γ is the reduction ratio of the gearhead, v_t is the speed constant of the motor, and t is the time required for moving such an angular displacement.

Fig.4 shows the process of target generation. The red dots, blue dots, orange dots and purple dots respectively represent the generated inside targets (I_target), outside targets (O_target), inside but inappropriate targets (II_target) and modified targets (M_target). The numbers signify the sequence of each target. The grey thick line represents the FWB. The blue imaginary lines and red lines are uncorrected trajectories UT and modified trajectories MT, respectively.

A new target will be randomly generated in the workspace of the device once the handle reaches it. As shown in Fig.4, the first target 1 (the followed targets will be called by sequence numbers for short) is a I_target, which is distinguished from O_target by a ray-based method. The link between P_s and 1 represents the first training trajectory. It is noteworthy that 2 is generated outside of the feasible workspace. To avoid the training trajectory beyond ROM of the participant, a M_target 3 being the intersection of the link from 1 to 2 and the FWB is utilized to replace 2. Similarly, the trajectory from 4 to 5 is substituted by the trajectory from 4 to 6. Although 6 and 7 are both located inside of the feasible workspace, a part of the link between 6 and 7 comes out through the feasible workspace due to irregularity. An analogous strategy is to find all the intersections of the link between 6 and 7 and the FWB, then select the closet one 8 as the modified target.

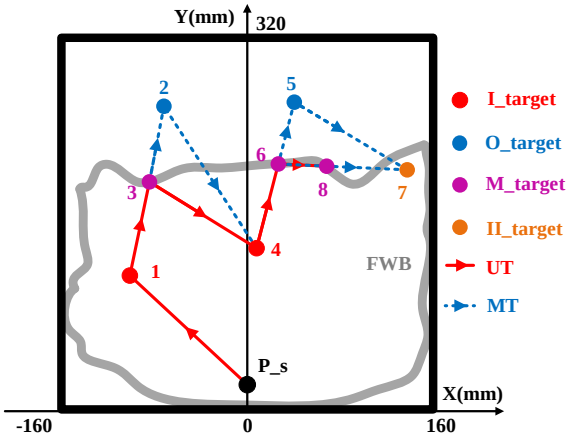

Fig.4: Target generation strategy. (The targets I_target and O_target represent targets generated inside and outside the feasible workspace. The target M_target is the modified target. The target II_target is the inappropriate target inside the feasible workspace. The grey thick line is the feasible workspace boundary FWB. The lines UT and MT respectively represent uncorrected trajectories and modified trajectories.)

The parameters Q_{thr}, Θ_{thr}, and T_{thr} are given by the virtual tunnels. To evaluate training performance, three indicators are used which are position deviation e_q from desired trajectory, angle deviation e_θ from desired angle θ_d, and time deviation e_t that has been applied by Lewis and Perreault [27]. More specifically, e_q and e_t are used to appraise the ability of moving ability, and e_θ is for coordinate ability estimation. It is defined that the position vector $q_{tar}^n = [X_{tar}^n \quad Y_{tar}^n]^T$ and $q_{tar}^{n+1} = [X_{tar}^{n+1} \quad Y_{tar}^{n+1}]^T$ are the n^{th} target and $(n+1)^{th}$ target. The parameter ${}^iq^n = [\,{}^iX^n, \ {}^iY^n]$ is the i^{th} sampling point of desired voluntary trajectory between these two dot targets. The parameter ${}^ie_q^n$ is the position deviation between ${}^iq^n$ and the desired trajectory (the line path between q_{tar}^n and q_{tar}^{n+1}). The position deviation value ${}^ie_q^n$ can be expressed in equations (4) to (7).

$${}^ie_q^n = \begin{cases} \frac{\left|A^n \ {}^iX^n + B^n \ {}^iY^n + C^n\right|}{\sqrt{(A^n)^2 + (B^n)^2}}, & {}^ie_q^n \le Q_{thr}, \ i=1,2,\ldots,N \\ Q_{thr}, & {}^ie_q^n > Q_{thr} \end{cases} \quad (4)$$

$$A^n = Y_{tar}^{n+1} - Y_{tar}^n \quad (5)$$

$$B^n = X_{tar}^n - X_{tar}^{n+1} \quad (6)$$

$$C^n = X_{tar}^{n+1} Y_{tar}^n - X_{tar}^n Y_{tar}^{n+1} \quad (7)$$

Then, the normalized position deviation e_q^n between q_{tar}^n and q_{tar}^{n+1} can be obtained based on (8),

$$e_q^n = \frac{1}{N} \sum_{i=1}^{N} {}^ie_q^n \quad (8)$$

where N is the sampling number between these two targets.

In a similar way, the measured angle of the i^{th} sampling point between q_{tar}^n and q_{tar}^{n+1} is denoted as ${}^i\theta^n$. The parameter ${}^ie_\theta^n$ is the angular deviation between ${}^i\theta^n$ and θ_d, and can be expressed in (9). Correspondingly, the normalized angle deviation between q_{tar}^n and q_{tar}^{n+1} can be obtained based on (10).

$${}^ie_\theta^n = \begin{cases} \left|\,{}^i\theta^n - \theta_d\right|, & {}^ie_\theta^n \le \Theta_{thr} \\ \Theta_{thr}, & {}^ie_\theta^n > \Theta_{thr} \end{cases}, i = 1,2,\ldots,N \quad (9)$$

$$e_\theta^n = \frac{1}{N} \sum_{j=1}^{N} {}^ie_\theta^n \quad (10)$$

It is defined that the desired complete time is t_d, and thus the measured time and time deviation between q_{tar}^n and q_{tar}^{n+1} are t^n and e_t^n, respectively, as in (11).

$$e_t^n = \begin{cases} t^n - t_d, e_t^n \le T_{thr} \\ T_t, e_t^n > T_{thr} \end{cases} \quad (11)$$

To standardize the range of e_p^n, e_θ^n and e_t^n, scaling to unit length strategy is used for feature scaling as shown in equation (12) to (14).

$$e_q^{n\prime} = \frac{e_q^n}{Q_{thr}} \quad (12)$$

$$e_\theta^{n\prime} = \frac{e_\theta^n}{\Theta_{thr}} \quad (13)$$

$$e_t^{n\prime} = \frac{e_t^n}{T_{thr}} \quad (14)$$

When subjects drive the robotic system under a high resistance level, it takes a longer time for them to reach the target. In this case the position and angle deviations are smaller. The adjustment value Δk^n during q_{tar}^n and q_{tar}^{n+1} can be described by weighting in equation (15),

$$\Delta k^n = \omega_q e_q^{n\prime} + \omega_\theta e_\theta^{n\prime} + \omega_t e_t^{n\prime} \quad (15)$$

where ω_q, ω_θ and ω_t are weights.

D. Subject-Specific Feasible Workspace

Miao, et al. [17] proposed a three-stage method to determine human hands' workspace on a subject-specific basis. This considered the human upper limb as a model with seven degrees of freedoms, and used the Denavit-Hartenberg method to derive the human hand workspace. In a similar way, the subject-specific workspace within the BULReD can be obtained, as presented in Fig.5. Part 1 shows the workspace of both hands based on a 175mm-height subject under the BULReD configuration, where W-R_hand represents the workspace of the right hand and W-L_hand for the left hand. The J-R_shoulder and J-L_shoulder represent the right and left shoulder joint, respectively. Due to the application for planar training, part 2 gives the workspace of hands on plane $Z = 0$. As shown in Fig.2, the subjects are asked to stay at desired angle θ_d, the workspace of the handle combined with hands workspace needs to be analyzed. For part 3, it indicates W-Device is the workspace of BULReD, and W-L_handle is the workspace of handle's left side. α is the intersection between W-L_handle and W-L_hand. Similarly, β is the intersection between W-R_handle and W-R_hand. It is defined β' is the handle's right-side workspace corresponding to α, which can be achieved by translating α. Then, the intersection $\varphi_\theta^r = \beta \cap \beta'$ is the handle's right-side feasible workspace, and the device feasible workspace φ_θ can be achieved in part 4 by φ_θ^r translation.

III. Experimental Results

A. Experiments

Five healthy subjects (three males: age 28.33±4.73 years, height 1786.70±40.41 mm, weight 86.33±3.21 kg, and two females: age 21.00±0.00 years, height 165.00±7.00 mm, weight 46.75±0.75 kg) volunteered to participate in this study. The study was approved by the University of Auckland, Human Participants Ethics Committee (019707) and consents were obtained from all participants. During the experiments, each participant was asked to actively reach 20 targets (not including P_s). These 20 targets randomly and sequentially appeared on the computer screen to direct the training inside the subject-specific workspace. In this study, the start point P_s and desired angle θ_d are set at $[0\ 20]$ and 45°, respectively. Three threshold values Q_{thr}, Θ_{thr} and T_{thr} are defined as 20mm, 10° and 5s, respectively. The parameter t_d is set as the time

completing the trajectories at a constant speed of 15mm/s. The weighting factors ω_q, ω_θ and ω_t are defined as 0.04, -0.02 and -0.04, respectively. Considering all the participants being healthy, the initial k^1 was set at 0.05.

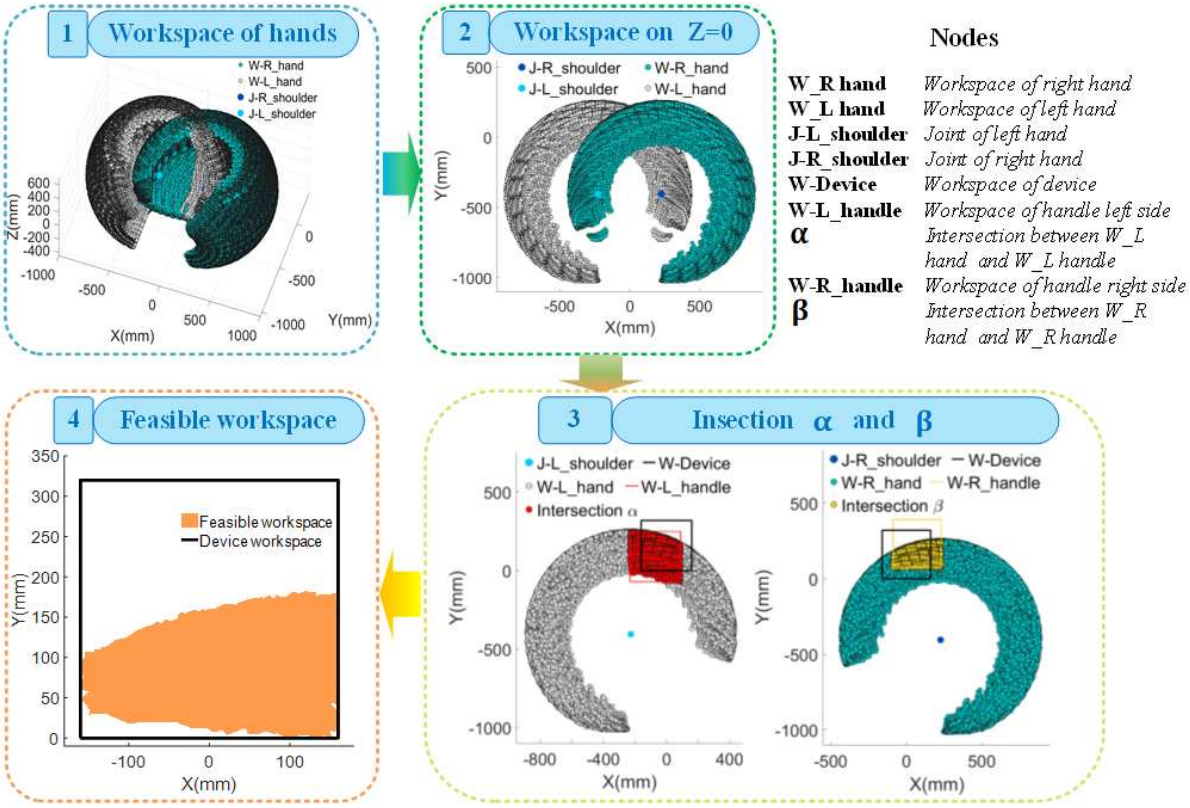

Fig.5 The process of subject-specific feasible workspace generation. (The generation sequence is from number 1 to 4.)

B. Results

Experimental results for the five healthy subjects are given in Fig.6 (a) to (e) corresponding to subjects (a) to (e). Each plot presents the FWB, random task targets, measured voluntary trajectory and desired voluntary trajectory. Fig.7 (a) presents desired voluntary and measured voluntary trajectories, in which blue, red, brown, green and purple lines match to subjects (a) to (e). Fig.7 (b) shows the trajectory tracking errors of the BULReD.

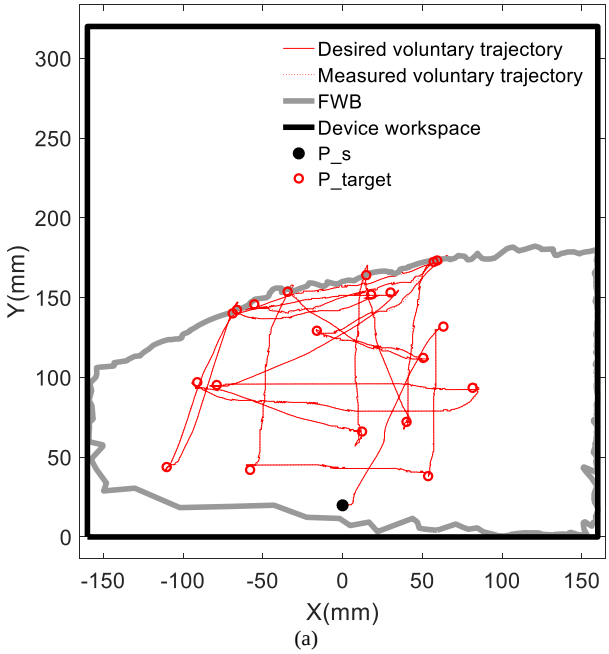

(a)

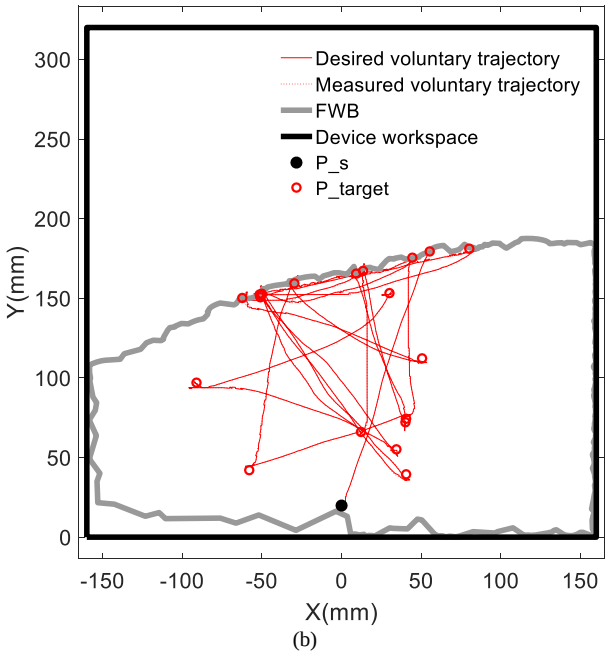

(b)

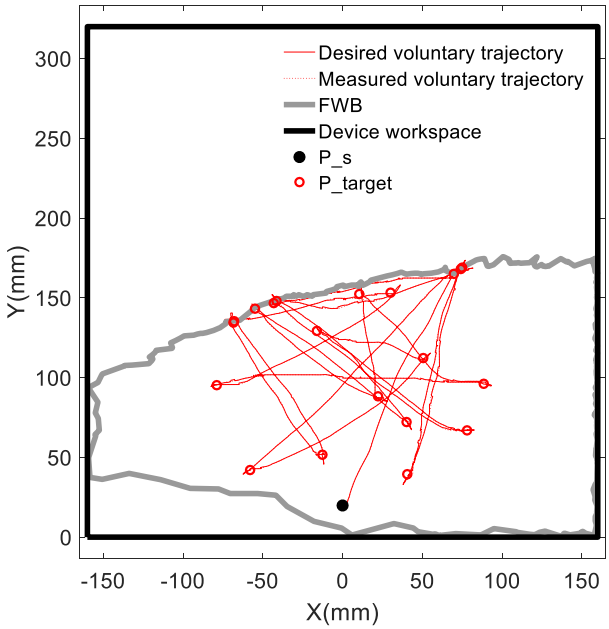

(c)

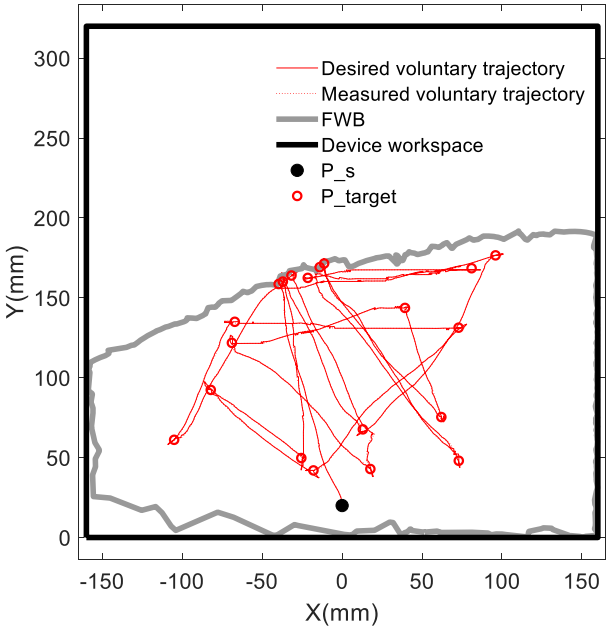

(d)

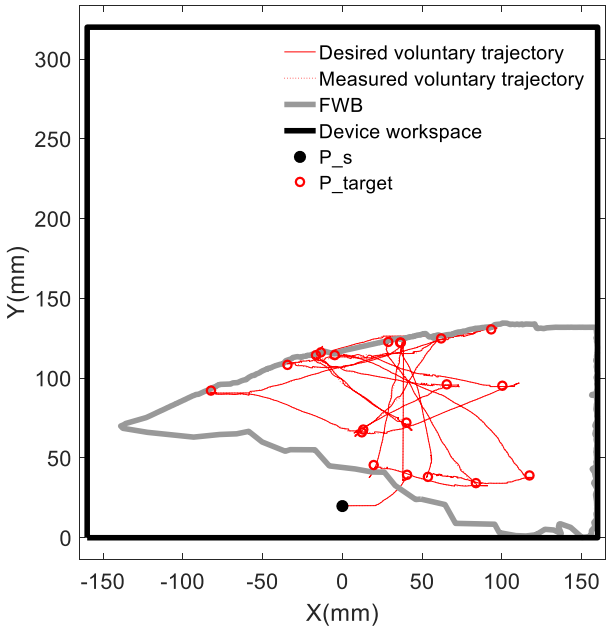

(e)

Fig.6: The total experimental results of every subject. (The figures (a) to (e) correspond to the results of subjects (a) to (e).)

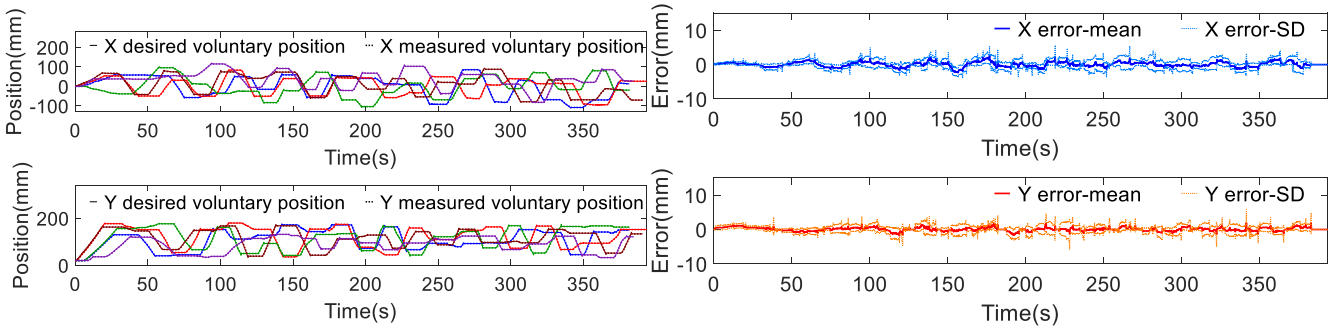

Fig.7: The trajectory tracking error. (a) represents the desired and measured voluntary trajectories, (b) represents the trajectory tracking error.

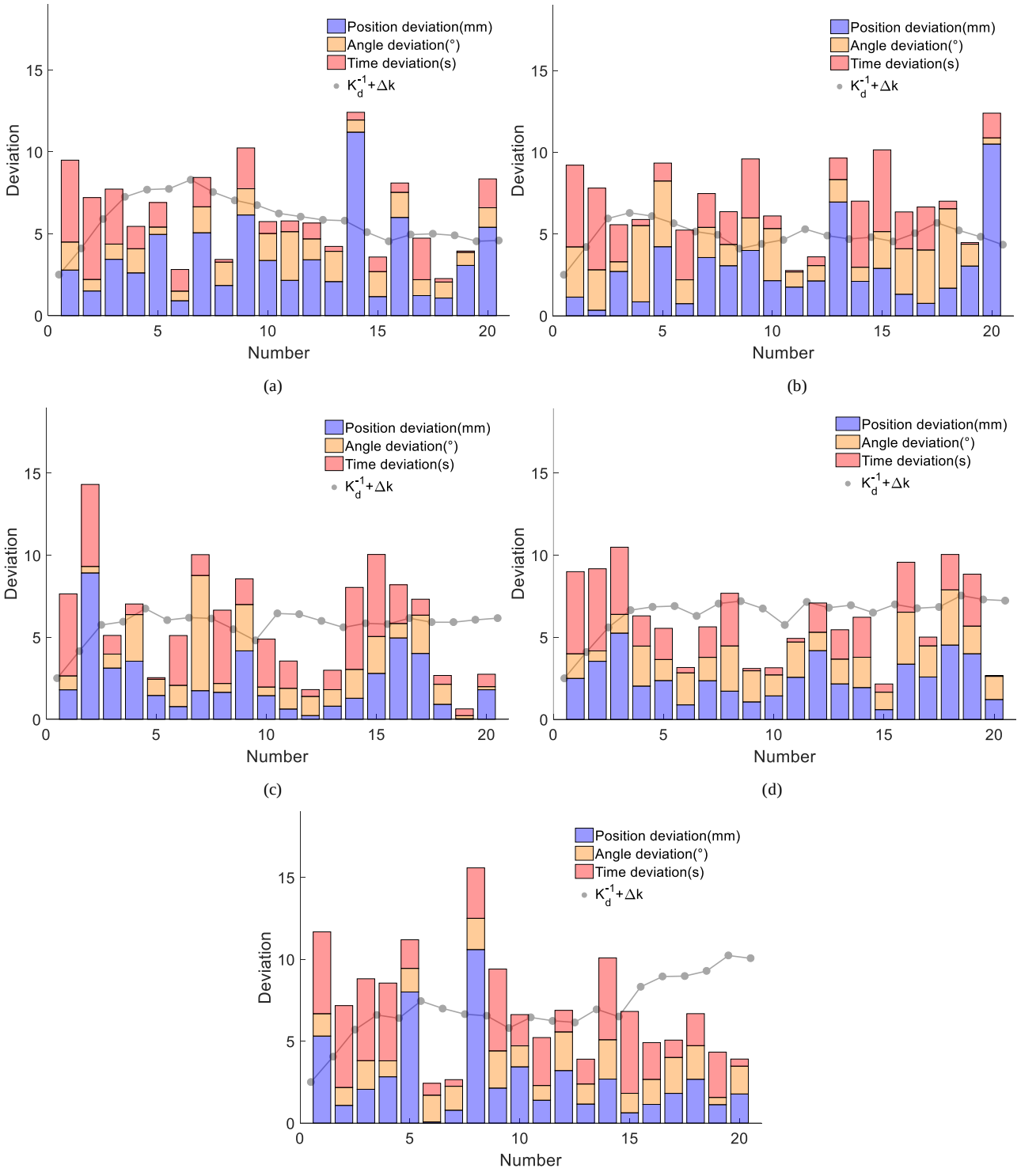

Fig.8: The results of performance evaluation and parameter adjustment. (The figures (a) to (e) correspond to the results of subjects (a) to (e)).

Statistical results of trajectory tracking performance are summarized in Table 1, where the mean values of root-mean-square error (RMSE) are 1.39mm and 1.21mm, respectively, for X-axis and Y-axis. The mean values of normalized root mean square error (NRMSE) on X-axis and Y-axis are 0.74% and 0.83%, respectively. These results show satisfactory trajectory tracking during robot-assisted bilateral upper limb training.

The performance evaluation of the five subjects and modified values $(K_d^{-1} + \Delta k)$ are given in Fig.8. To make it clearer to analyze the relevance, the $(K_d^{-1} + \Delta k)$ value are multiplied by 50. It can be seen that the modified values $(K_d^{-1} + \Delta k)$ vary a lot during the first 10 or 12 training rounds but slightly change for last 10 or 8 rounds in Figs 8 (a)-(d). This can

be accounted by that subjects (a) to (d) tried to adapt to training tasks in early stage, and became familiar for last 10 or 8 rounds. More specifically, the modified values $(K_d^{-1} + \Delta k)$ of subject (b) still varies obviously during the last 10 rounds, which may suggest a longer slower adaptation to task difficulty. Differently, the data presented in Fig.8 (e) show continuous rise of the $(K_d^{-1} + \Delta k)$ value, either in the first 5 rounds or the last 5 rounds. However, it is worth mentioning that subject (e) reported her tired arms during the second-half stage and failed to focus on the completion of training tasks. This can be the reason why the $(K_d^{-1} + \Delta k)$ values of subject (e) do not flatten during the late stage of the training tasks.

Table 1 Statistical results of trajectory tracking performance.

No.	X-axis		Y-axis	
	RMSE (mm)	NRMSE (%)	RMSE (mm)	NRMSE (%)
(a)	1.44	0.74	1.20	0.79
(b)	1.36	0.76	1.26	0.79
(c)	1.42	0.85	1.27	0.86
(d)	1.33	0.66	1.42	0.91
(e)	1.38	0.70	0.89	0.80
Mean	1.39	0.74	1.21	0.83

IV. DISCUSSION

Robot-assisted bilateral upper limb training is an emerging form of stroke rehabilitation. Most of previous studies used joint space symmetry (mirror) training and visual symmetry modes based on two robotic devices or one device with an external element [14-17, 19]. It is worth mentioning that using multiple devices makes the training system more complex and expensive. There are two typical one-device-two-handle robotic systems specially designed for cooperation and coordination training of bilateral limbs, with one developed by Trlep, et al. [22] and one by Squeri, et al. [23]. Trlep, et al. [22] reduced the force provided by the healthy limb to imitate the impaired limb's movement. Squeri, et al. [23] adjusted the amount of assistance based on a force field. However, providing too much assistance has negative consequences [28], and encouraging engagement from human users may lead to better training efficacy. This suggests assisting participants only as much as needed according to their real-time training performance.

To increase patients' engagement, assist-as-needed (AAN) algorithms are proposed to achieve better bilateral upper limb training effectiveness [29, 30]. Harischandra and Abeykoon [29] proposed a novel impedance controlled bimanual robot with fuzzy logic based adaptive assistance. The AAN controller was designed using a simple proportional controller with a fuzzy regulator for gain scheduling, which can provide assistance torque based on patient's ability to coordinating his/her arms. Shahbazi, et al. [30] proposed a therapist-in-the-loop framework for robotics-assisted mirror rehabilitation integrated with adaptive assist-as-needed therapy. The framework used a patient's functional limb as the medium to transfer therapeutic training from the therapist to the patient's impaired limb. It implemented two motor function assessment metrics to provide objective assessment of the impaired limb's motor deficiency. It also and presented an adaptation law to adjust the intensity of the therapy delivered to the patient in real time and based on the aforementioned estimation of the impairment level of the impaired limb. However, the so-called "slacking" principle exists once patients adapt to the provided assistance, which can negatively affect rehabilitation efficiency"

The proposed robot-assisted bilateral upper limb training strategy overcomes the above-mentioned limitation of continuous assistance. It enables participants to independently complete a task session instead of real-time assistance or resistance. Its control parameters are adjusted on a session by session basis, rather than in real-time. This may lead to two major advantages: 1) continuously challenging patients and thus encouraging more active engagement with training tasks; and 2) helping with identifying the most appropriate training protocol in terms of task execution time, determination of the optimal training path tunnel and pose angle tunnel.

Another benefit of the proposed training strategy is the safe and effective workspace determination on a subject-specific basis. Previous studies generally used the healthy arm to guide the injured side based on the healthy limb workspace [15, 19, 31]. It should be noted that the use of the healthy side workspace may be unsafe for the training of injured limbs due to their reduced range of motion. In contrast, this study developed an appropriate workspace on an individual basis using a three-stage workspace determination method [17], as detailed in Fig. 5. This method relies on preliminary assessment of the human use's joint range of motion, and thus the derived subject-specific workspace can ensure the training safety. However, it should be noted that the proposed strategy works better in a normal condition, rather than when human users start feeling extremely tired and is physically unable to conduct tasks.

While the proposed bilateral training strategy has been validated with five healthy subjects, this study suffers from some limitations. First, this study defines training tasks only in a two-dimensional space, while actual activities of daily living generally happen in a three-dimensional space. Second, the weighting factors used for controller tuning are defined out of experience, and thus optimization techniques could be involved for optimal control performance. Third, only five healthy subjects were recruited as a preliminary evaluation of the proposed training strategy, and a larger sample of people with reduced upper limb workspace due to a disability should be involved. Fourth, the presented strategy still needs some modifications before clinical applications on patients with upper limb disabilities, such as enhanced training safety measures and more comprehensive training performance evaluation indexes.

V. CONCLUSION

This paper proposes a new robot-assisted bilateral upper limb training strategy, focusing on the coordination training of human users' bilateral upper limbs. Its implementation within subject-specific feasible workspace contributes to enhanced training safety, and an adaptive stiffness adjustment algorithm assists participants in completing training tasks at an appropriate difficulty level. Experimental results demonstrate that the proposed training strategy requires significant coordination of human users' bilateral upper limbs for task completion, indicating it has potential for clinical application. Future work will increase the number of participants for training experiments, and focus on the presented strategy's clinical evaluation on patients with upper limb disabilities. This strategy will also be investigated for lower limb rehabilitation.

References

[1] G. Kwakkel, B. J. Kollen, J. van der Grond, and A. J. H. Prevo, "Probability of Regaining Dexterity in the Flaccid Upper Limb," Impact of Severity of Paresis and Time Since Onset in Acute Stroke, vol. 34, no. 9, pp. 2181-2186, 2003.

[2] E. Taub et al., "Technique to improve chronic motor deficit after stroke," (in eng), Archives of physical medicine and rehabilitation, vol. 74, no. 4, pp. 347-354, 1993/04// 1993.

[3] J. Whitall, S. M. Waller, K. H. C. Silver, and R. F. Macko, "Repetitive Bilateral Arm Training With Rhythmic Auditory Cueing Improves Motor Function in Chronic Hemiparetic Stroke," Stroke, vol. 31, no. 10, pp. 2390-2395, 2000.

[4] Y. Ren, S. H. Kang, H.-S. Park, Y.-N. Wu, and L.-Q. Zhang, "Developing a multi-joint upper limb exoskeleton robot for diagnosis, therapy, and outcome evaluation in neurorehabilitation," IEEE Transactions on Neural Systems and Rehabilitation Engineering, vol. 21, no. 3, pp. 490-499, 2013.

[5] A. Van Delden, C. L. E. Peper, G. Kwakkel, and P. J. Beek, "A systematic review of bilateral upper limb training devices for poststroke rehabilitation," Stroke research and treatment, vol. 2012, 2012.

[6] J. Brackenridge, L. V Bradnam, S. Lennon, J. J Costi, and D. A Hobbs, "A Review of Rehabilitation Devices to Promote Upper Limb Function Following Stroke," Neuroscience and Biomedical Engineering, vol. 4, no. 1, pp. 25-42, 2016.

[7] H. S. Lo and S. Q. Xie, "Exoskeleton robots for upper-limb rehabilitation: State of the art and future prospects," Medical engineering & physics, vol. 34, no. 3, pp. 261-268, 2012.

[8] T. Proietti, V. Crocher, A. Roby-Brami, and N. Jarrassé, "Upper-limb robotic exoskeletons for neurorehabilitation: a review on control strategies," IEEE reviews in biomedical engineering, vol. 9, pp. 4-14, 2016.

[9] K. K. Ang et al., "A randomized controlled trial of EEG-based motor imagery brain-computer interface robotic rehabilitation for stroke," Clinical EEG and neuroscience, vol. 46, no. 4, pp. 310-320, 2015.

[10] V. Klamroth-Marganska et al., "Three-dimensional, task-specific robot therapy of the arm after stroke: a multicentre, parallel-group randomised trial," The Lancet Neurology, vol. 13, no. 2, pp. 159-166, 2014.

[11] J. J. Summers, F. A. Kagerer, M. I. Garry, C. Y. Hiraga, A. Loftus, and J. H. Cauraugh, "Bilateral and unilateral movement training on upper limb function in chronic stroke patients: a TMS study," Journal of the neurological sciences, vol. 252, no. 1, pp. 76-82, 2007.

[12] M. E. Stoykov, G. N. Lewis, and D. M. Corcos, "Comparison of bilateral and unilateral training for upper extremity hemiparesis in stroke," Neurorehabilitation and neural repair, vol. 23, no. 9, pp. 945-953, 2009.

[13] F. Debaere, N. Wenderoth, S. Sunaert, P. Van Hecke, and S. P. Swinnen, "Changes in brain activation during the acquisition of a new bimanual coordination task," Neuropsychologia, vol. 42, no. 7, pp. 855-867, 2004/01/01/ 2004.

[14] S. Guo, W. Zhang, W. Wei, J. Guo, Y. Ji, and Y. Wang, "A kinematic model of an upper limb rehabilitation robot system," in Mechatronics and Automation (ICMA), 2013 IEEE International Conference on, 2013, pp. 968-973: IEEE.

[15] E. Rashedi, A. Mirbagheri, B. Taheri, F. Farahmand, G. Vossoughi, and M. Parnianpour, "Design and development of a hand robotic rehabilitation device for post stroke patients," in Engineering in Medicine and Biology Society, 2009, pp. 5026-5029: IEEE.

[16] J. W. Stinear and W. D. Byblow, "Rhythmic bilateral movement training modulates corticomotor excitability and enhances upper limb motricity poststroke: a pilot study," Journal of Clinical Neurophysiology Official Publication of the American Electroencephalographic Society, vol. 21, no. 2, p. 124, 2004.

[17] Q. Miao, A. McDaid, M. Zhang, P. Kebria, and H. Li, "A three-stage trajectory generation method for robot-assisted bilateral upper limb training with subject-specific adaptation," Robotics and Autonomous Systems, vol. 105, pp. 38-46, 2018.

[18] P. S. Lum, D. J. Reinkensmeyer, and S. L. Lehman, "Robotic assist devices for bimanual physical therapy: preliminary experiments," IEEE Transactions on Rehabilitation Engineering, vol. 1, no. 3, pp. 185-191, 1993.

[19] D. Leonardis et al., "An EMG-controlled robotic hand exoskeleton for bilateral rehabilitation," IEEE transactions on haptics, vol. 8, no. 2, pp. 140-151, 2015.

[20] W.-M. Lien, H.-Y. Li, H.-Y. Hong, S.-H. Chen, L.-C. Fu, and J.-S. Lai, "Developing a novel bilateral arm training on rehabilitation robot NTUH-II for neurologic and orthopedic disorder," in Robotics and Biomimetics (ROBIO), 2015 IEEE International Conference on, 2015, pp. 158-163: IEEE.

[21] M. J. Johnson, H. M. Van der Loos, C. G. Burgar, P. Shor, and L. J. Leifer, "Experimental results using force-feedback cueing in robot-assisted stroke therapy," IEEE Transactions on Neural Systems and Rehabilitation Engineering, vol. 13, no. 3, pp. 335-348, 2005.

[22] M. Trlep, M. Mihelj, U. Puh, and M. Munih, "Rehabilitation robot with patient-cooperative control for bimanual training of hemiparetic subjects," Advanced Robotics, vol. 25, no. 15, pp. 1949-1968, 2011.

[23] V. Squeri, M. Casadio, E. Vergaro, P. Giannoni, P. Morasso, and V. Sanguineti, "Bilateral robot therapy based on haptics and reinforcement learning: Feasibility study of a new concept for treatment of patients after stroke," Journal of rehabilitation medicine, vol. 41, no. 12, pp. 961-965, 2009.

[24] S. McAmis and K. B. Reed, "Symmetry modes and stiffnesses for bimanual rehabilitation," in Rehabilitation Robotics (ICORR), 2011 IEEE International Conference on, 2011, pp. 1-6: IEEE.

[25] Q. Miao, M. Zhang, Y. Wang, and S. Q. Xie, "Design and Interaction Control of a New Bilateral Upper Limb Rehabilitation Device (BULReD)."

[26] D. A. Winter, "Biomechanics and Motor Control of Human Movement," Physiotherapy, vol. 74, no. 2, pp. 94-94, 1990.

[27] G. N. Lewis and E. J. Perreault, "An assessment of robot-assisted bimanual movements on upper limb motor coordination following stroke," IEEE Transactions on Neural Systems and Rehabilitation Engineering, vol. 17, no. 6, pp. 595-604, 2009.

[28] L. Marchal-Crespo and D. J. Reinkensmeyer, "Review of control strategies for robotic movement training after neurologic injury," Journal of NeuroEngineering and Rehabilitation, journal article vol. 6, no. 1, p. 20, 2009.

[29] P. D. Harischandra and A. H. S. Abeykoon, "Intelligent bimanual rehabilitation robot with fuzzy logic based adaptive assistance," International Journal of Intelligent Robotics and Applications, vol. 3, no. 1, pp. 59-70, 2019.

[30] M. Shahbazi, S. F. Atashzar, M. Tavakoli, and R. V. Patel, "Robotics-assisted mirror rehabilitation therapy: a therapist-in-the-loop assist-as-needed architecture," IEEE/ASME Transactions on Mechatronics, vol. 21, no. 4, pp. 1954-1965, 2016.

[31] C. Li, Y. Inoue, T. Liu, K. Shibata, and K. Oka, "A new master-slave control method for implementing force sensing and energy recycling in a bilateral arm training robot," International Journal of Innovative Computing, Information and Control, vol. 7, no. 1, pp. 471-485, 2011.